PHYSICAL REVIEW C **91**, 062501(R) (2015)

Electromagnetic and neutral-weak response functions of ^{4}He and ^{12}C

A. Lovato,[1,2] S. Gandolfi,[3] J. Carlson,[3] Steven C. Pieper,[2] and R. Schiavilla[4,5]

[1]*Argonne Leadership Computing Facility, Argonne National Laboratory, Argonne, Illinois 60439, USA*

[2]*Physics Division, Argonne National Laboratory, Argonne, Illinois 60439, USA*

[3]*Theoretical Division, Los Alamos National Laboratory, Los Alamos, New Mexico 87545, USA*

[4]*Theory Center, Jefferson Lab, Newport News, Virginia 23606, USA*

[5]*Department of Physics, Old Dominion University, Norfolk, Virginia 23529, USA*

(Received 19 January 2015; published 4 June 2015)

Background: A major goal of nuclear theory is to understand the strong interaction in nuclei as it manifests itself in terms of two- and many-body forces among the nuclear constituents, the protons and neutrons, and the interactions of these constituents with external electroweak probes via one- and many-body currents.

Purpose: The objective of the present work is to calculate the quasielastic electroweak response functions in light nuclei within the realistic dynamical framework outlined above. These response functions determine the inclusive cross section as function of the lepton momentum and energy transfers.

Methods: Their *ab initio* calculation is a very challenging quantum many-body problem, since it requires summation over the entire excitation spectrum of the nucleus and inclusion in the electroweak currents of one- and many-body terms. Green's functions Monte Carlo methods allow one to circumvent both difficulties by computing the response in imaginary time (the so-called Euclidean response) and hence summing implicitly over the bound and continuum states of the nucleus, and by implementing specific algorithms designed to deal with the complicated spin-isospin structure of nuclear many-body operators.

Results: Theoretical predictions for ^{4}He and ^{12}C, confirmed by experiment in the electromagnetic case, show that two-body currents generate excess transverse strength from threshold to the quasielastic to the dip region and beyond.

Conclusions: These results challenge the conventional picture of quasielastic inclusive scattering as being largely dominated by single-nucleon knockout processes.

DOI: 10.1103/PhysRevC.91.062501 PACS number(s): 21.60.De, 25.30.Pt, 27.10.+h, 27.20.+n

In first-order perturbation theory, the interactions of an external electroweak probe with a nucleus are described by response functions, which encode the strong-interaction dynamics of the nuclear constituents, the protons and neutrons, and their coupling to these external fields. The response functions—two for the electromagnetic processes $A(e,e')$, and five for the neutral or charge-changing weak processes $A(\nu_l,\nu_l')$ and $A(\overline{\nu}_l,\overline{\nu}_l')$, or $A(\nu_l,l^-)$ and $A(\overline{\nu}_l,l^+)$—determine the inclusive differential cross sections [1]. They can be written schematically as

$$R_{\alpha\beta}(q,\omega) \sim \sum_f \delta(\omega + E_0 - E_f)\langle f|O_\alpha(\mathbf{q})|0\rangle^* \times\langle f|O_\beta(\mathbf{q})|0\rangle, \tag{1}$$

where $\mathbf{q}$ and ω are the momentum and energy transfers injected by the external field into the nucleus, $|0\rangle$ and $|f\rangle$ represent respectively its initial ground state of energy E_0 and final continuum state of energy E_f (a sum over these continuum states is implied), $O_\alpha(\mathbf{q})$ and $O_\beta(\mathbf{q})$ denote appropriate components of the nuclear electroweak current operator (see Supplemental Material [2]) (their ω dependence is dealt with as described below), and an average over the ground-state spin projections is understood (precise definitions for the nuclear electroweak response functions, and resulting inclusive cross sections, are given in Ref. [1]).

At large values of momentum and energy transfers ($q \gtrsim 1$ GeV and $\omega \gtrsim 0.5$ GeV), where the dynamics of interacting nucleons is inextricably interwoven with the internal dynamics of individual nucleons, the accurate calculation of the response functions poses formidable challenges, particularly in view of the fact that a consistent framework to describe such a regime in QCD is still lacking. Even at the lower q and ω of interest in the present study ($q \lesssim 0.5$ GeV and ω in the quasielastic region), where the consequences of the nucleon's substructure on nuclear dynamics can be subsumed into effective many-body potentials and currents, this calculation remains extremely difficult: it requires summation over the entire excitation spectrum of the nucleus and inclusion in the electroweak currents of one- and many-body terms.

In the case of inclusive weak scattering, a further difficulty exists for comparing calculated and experimental results. Because neutrino beams are produced as secondary decay products, their energy is not sharply defined, but broadly distributed. This means that the observed cross section for a given energy and angle of the final lepton follows from a folding with the energy distribution of the incoming neutrino flux and, consequently, may include contributions from q-ω regions where different mechanisms are at play: the threshold region, where the structure of the low-lying energy spectrum and collective effects are important; the quasielastic region, which is dominated by scattering off individual nucleons and nucleon pairs (see below); and the Δ-resonance region, where one or more pions are produced in the final state [3].

Integral properties of the response functions can be studied by means of sum rules, which are obtained from ground-state expectation values of appropriate combinations of the current operators (and commutators of these combinations with the Hamiltonian in the case of energy-weighted sum rules), thus avoiding the need for computing the nuclear excitation spectrum. *Ab initio* quantum Monte Carlo (QMC) calculations of (non-energy-weighted) electroweak sum rules in ^{12}C have been recently reported in Refs. [4,5]. These calculations have demonstrated that a large fraction ($\simeq$30%) of the strength in the response arises from processes involving two-body currents, and that interference effects between the matrix elements of one- and two-body currents play a major role [6]. These effects are typically only partially, or approximately, accounted for in existing perturbative or mean-field studies [7–10].

However, sum rules do not provide direct information on the distribution of strength, whether, for example, the calculated excess strength induced by two-body currents is mostly at large ω, well beyond the quasielastic peak energy $\omega_{\rm qe} = \sqrt{q^2+m^2} - m$ (m is the nucleon mass), or is also found in the quasielastic region with $\omega \lesssim \omega_{\rm qe}$. Moreover, in the electromagnetic case, comparison of theoretical and experimental sum rules is problematic, since longitudinal and transverse response functions obtained from Rosenbluth separation of measured inclusive (e,e') cross sections are only available in the space-like region ($\omega < q$) and therefore must be extrapolated into the unobserved time-like region ($\omega > q$) before "experimental" values for the sum rules can be determined; see Refs. [4,11] for a discussion of these issues.

In this paper we report the first *ab initio* calculations of the electromagnetic and neutral-weak response functions of ^{4}He and ^{12}C (other studies for ^{4}He have been already performed within different frameworks, see Refs. [12–14]). These calculations proceed in two steps: the first involves the use of QMC methods to compute the response in imaginary time, the so-called Euclidean response [15,16], while the second consists in the inversion, via maximum-entropy techniques [17,18], of these "noisy" imaginary-time data to obtain $R_{\alpha\beta}(q,\omega)$. The dynamical framework is based on a realistic Hamiltonian, including the Argonne v_{18} two-nucleon [19] (AV18) and Illinois-7 three-nucleon [20] (IL7) potentials, and on realistic electroweak currents with one- and two-body terms. A concise description of this framework is in Refs. [4,5], while a more extended one can be found in the reviews [21,22]. These latter papers also illustrate the level of quantitative success that has been achieved in accurately predicting many properties of s- and p-shell nuclei up to ^{12}C, including, among others, energy spectra of low-lying states, static properties like charge radii, magnetic dipole and electric quadrupole moments, radiative and weak transition rates, and elastic and inelastic electromagnetic form factors.

The Euclidean response function is defined as the Laplace transform of the response

$$E_{\alpha\beta}(q,\tau) = C_{\alpha\beta}(q) \int_{\omega_{\rm th}}^{\infty} d\omega\, e^{-\tau\omega} R_{\alpha\beta}(q,\omega) , \qquad (2)$$

where $\omega_{\rm th}$ is the inelastic threshold and the $C_{\alpha\beta}$ are q-dependent normalization factors. In $R_{\alpha\beta}(q,\omega)$ the ω dependence enters via the energy-conserving δ function and the dependence on the four-momentum transfer $Q^2 = q^2 - \omega^2$ of the electroweak form factors of the nucleon and N-to-Δ transition in the currents. We remove the latter by evaluating these form factors at $Q^2_{\rm qe} = q^2 - \omega^2_{\rm qe}$ (we have explicitly verified that this approximation leads to a negligible correction in the deuteron). In the case of the electromagnetic longitudinal (L or $\alpha\beta = 00$) and transverse (T or $\alpha\beta = xx$) response functions, the normalization factors are [11] $C_L = C_T = 1/[G_E^p(Q^2_{\rm qe})]^2$, where G_E^p is the proton electric form factor, while in the neutral-weak response functions they are the same as those adopted in the sum rule calculations reported in Ref. [5]. With these definitions the response functions in Eq. (2) can be thought of as being due to point-like, but strongly interacting, nucleons. Note that non-energy-weighted sum rules correspond to $E_{\alpha\beta}(q,\tau=0)$, while energy-weighted ones are obtained by taking derivatives of $E_{\alpha\beta}(q,\tau)$ with respect to τ and evaluating them at $\tau = 0$.

The Euclidean response can be expressed as a ground-state expectation value,

$$\frac{E_{\alpha\beta}(q,\tau)}{C_{\alpha\beta}(q)} = \frac{\langle 0|O^\dagger_\alpha(\mathbf{q}) e^{-(H-E_0)\tau} O_\beta(\mathbf{q})|0\rangle}{\langle 0|e^{-(H-E_0)\tau}|0\rangle} , \qquad (3)$$

where H is the nuclear Hamiltonian (here, the AV18 + IL7 model), τ is the imaginary time, and E_0 is a trial energy to control the normalization. In this paper we report responses computed with the variational wave function, $|0\rangle = |\Psi_V\rangle$; in Refs. [4,5] it was shown that sum rules computed with $|\Psi_V\rangle$ for ^{12}C are very close (within less than 5%) to those computed with the exact Green's function Monte Carlo (GFMC) wave function. The calculation of the matrix element above is carried out with GFMC methods [15] similar to those used in projecting out the exact ground state of H from a trial state [23]. It proceeds in two steps. First, an unconstrained imaginary-time propagation of the variational Monte Carlo (VMC) state $|\Psi_V\rangle$ is performed and saved. Next, the states $O_\beta(\mathbf{q})|\Psi_V\rangle$ are evolved in imaginary time following the path previously saved. During this latter imaginary-time evolution, scalar products of $\exp[-(H-E_0)\tau_i]O_\beta(\mathbf{q})|\Psi_V\rangle$ with $O_\alpha(\mathbf{q})|\Psi_V\rangle$ are evaluated on a grid of τ_i values, and from these scalar products estimates for $E_{\alpha\beta}(q,\tau_i)$ are obtained (a complete discussion of the methods is in Refs. [11,15]).

In Fig. 1 the electromagnetic longitudinal (E_L, top panel) and transverse (E_T, lower panel) Euclidean response functions of ^{12}C are compared to those obtained from the world data analysis by Jourdan [24], represented by the shaded bands. In order to better show the large τ behavior, all the figures in this paper show $\widetilde{E}_{\alpha\beta}(q,\tau) = \exp[\tau\, q^2/(2m)]E_{\alpha\beta}(q,\tau)$; this scaled response would be a constant for an isolated proton. The "experimental" $E_L(q,\tau)$ and $E_T(q,\tau)$ follow from Laplace-transforming the longitudinal and transverse data. These are first divided by $[G_E^p(Q^2)]^2$ to obtain corresponding response functions of point-like nucleons, and then integrated with the weight factor $\exp(-\tau\omega)$ up to $\omega_{\rm max}$, where measurements are available. The strength in the unobserved region with $\omega > \omega_{\rm max}$ is estimated by assuming that the $R_L(q,\omega > \omega_{\rm max})$ and $R_T(q,\omega > \omega_{\rm max})$ of ^{12}C are proportional to those in the deuteron, which can be accurately calculated [1]. The procedure is identical to that used in Ref. [4] for the sum rules. As discussed in Ref. [4], the scaling assumption can be justified by observing that the high ω (well beyond $\omega_{\rm qe}$) region of the response is dominated by two-nucleon physics, in particular by deuteron-like np pairs in the ground state of the nucleus. It is important to stress that, as τ increases, the Euclidean response functions become more and more sensitive to strength in the quasielastic and threshold regions of $R_{L,T}(q,\omega)$. Indeed, in this limit ($\tau \gtrsim 1/\omega_{\rm qe}$) contributions from unmeasured strength at $\omega > \omega_{\rm max}$ are exponentially suppressed.

In Fig. 1 we show results obtained by including only one-body (open circles) or both one- and two-body (solid circles) terms in the electromagnetic transition operators. In the longitudinal case, destructive interference between the matrix elements of the one- and two-body charge operators reduces, albeit slightly, the one-body response. In the transverse case, on the other hand, two-body current contributions substantially increase the one-body response. This enhancement is effective over the whole imaginary-time region we have considered, with the implication that excess transverse strength is generated by two-body currents not only at $\omega \gtrsim \omega_{\rm qe}$, but also in the quasielastic and threshold regions of $R_T(q,\omega)$. It is reassuring to see that the full predictions for both longitudinal and transverse Euclidean response functions are in excellent agreement with data.

At larger values of τ the statistical errors associated with the GFMC evolution are rather large, particularly in the longitudinal response for which the elastic contribution proportional to the square of the ^{12}C form factor [4] is removed in order to account for the inelastic strength only. However, it should be possible to reduce these errors in the future by investing substantial additional computational resources in this

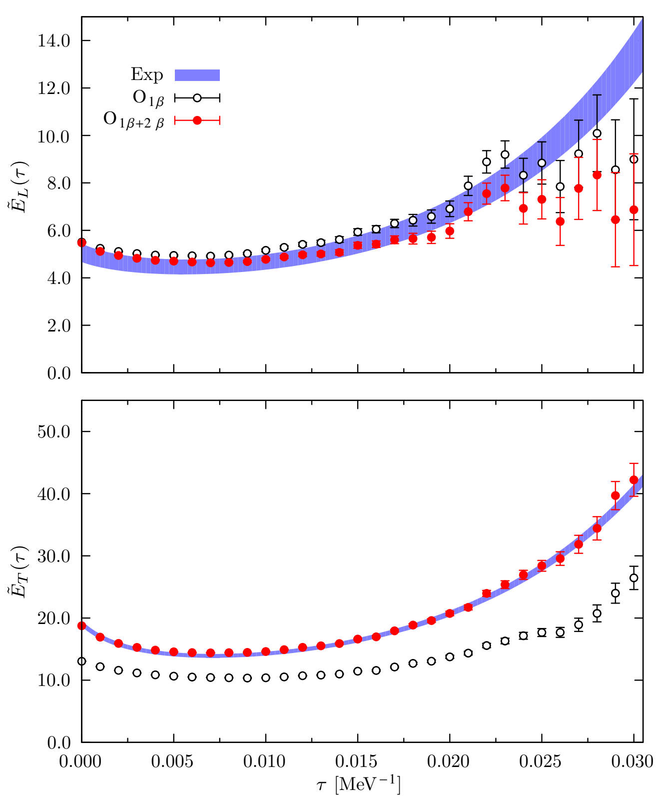

FIG. 1. (Color online) Euclidean electromagnetic longitudinal (top panel) and transverse (lower panel) response function of ^{12}C at $q = 570$ MeV. Experimental data are from Ref. [24].

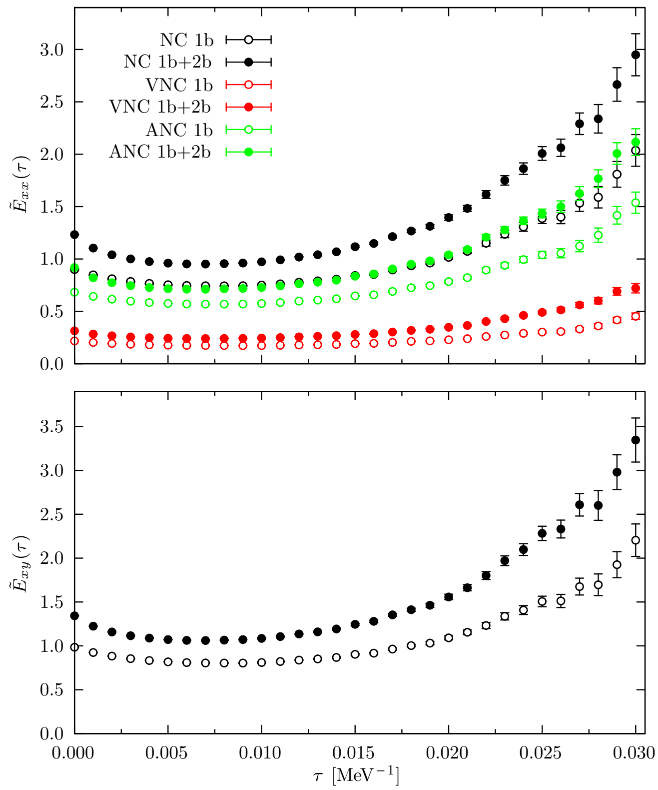

FIG. 2. (Color online) Euclidean neutral-weak transverse (top panel) and interference (lower panel) response functions ($\alpha\beta = xx$ and xy in the notation of Ref. [1]) of ^{12}C at $q = 570$ MeV. See text for further explanations.

type of calculation. Those presented here were performed with ~45 million core hours of Argonne National Laboratory's IBM Blue Gene/Q (Mira) parallel supercomputer. The Automatic Dynamic Load Balancing (ADLB) library [25] was used to distribute the imaginary time propagation of $O_\beta(\mathbf{q})|\Psi_V\rangle$ and the evaluation of the matrix element in Eq. (3) over more than 8000 nodes. The code is at present approximately 75% efficient at this scale.

In Fig. 2 we show the largest of the five Euclidean neutral-weak response functions: the transverse (top panel) and interference (lower panel) $E_{\alpha\beta}(q,\tau)$, having respectively $\alpha\beta = xx$ and $\alpha\beta = xy$ in the notation of Ref. [1]. The $E_{xy}(q,\tau)$ response is due to interference between the vector (VNC) and axial (ANC) parts of the neutral current (NC), and in the inclusive cross section the corresponding $R_{xy}(q,\omega)$ enters with opposite sign depending on whether the process $A(\nu_l,\nu_l')$ or $A(\overline{\nu}_l,\overline{\nu}_l')$ is considered [1]—the difference between the $\sigma(\nu)$ and $\sigma(\overline{\nu})$ cross sections is proportional to R_{xy}. It is important to note that this difference will have an impact on the determination of the CP-violating phase extracted from $A(\nu_l,\nu_l')$ and $A(\overline{\nu}_l,\overline{\nu}_l')$ scattering experiments at DUNE [26].

On the other hand, in the transverse case the interference of VNC and ANC terms vanishes, and $E_{xx}(q,\tau)$ is simply given by the sum of the terms with both O_α and O_β in Eq. (1) being from the VNC or from the ANC. For $E_{xx}(q,\tau)$ these individual contributions, along with their sum, are displayed separately. Both $E_{xx}(q,\tau)$ and $E_{xy}(q,\tau)$ response functions obtained with one-body terms only in the NC are substantially increased when two-body terms are also retained. This enhancement is found not only at low τ, thus corroborating the sum-rule predictions of Ref. [5], but in fact also extends over the whole τ region studied here. Moreover, in the case of the transverse response, it affects, in relative terms, the individual (VNC-VNC) and (ANC-ANC) contributions about equally.

The VNC consists of a linear combination of the isoscalar and isovector components of the electromagnetic current, weighted respectively by the factors $-2\sin^2\theta_W$ and $(1-2\sin^2\theta_W)$ with θ_W being the Weinberg angle. The excess transverse strength induced by two-body terms in the VNC is consistent with that found in the transverse electromagnetic response, and is confirmed by experiment as Fig. 1 demonstrates. The two-body enhancement in the (ANC-ANC) contribution of $E_{xx}(q,\tau)$ is substantial at these relatively large q's. It decreases significantly (for $\tau \gtrsim 0.01$ MeV^{-1}) as q is reduced [27], consistently with what is found in calculations of low q charge-changing weak transitions to specific low-lying states, such as the β decays and electron and muon captures studied in Refs. [28,29], where it amounts to a few percent. In principle, the enhancement in the quasielastic region could be measured in parity-violating inclusive $(\vec{e},e')$ scattering at backward angles. However, the smallness of the factor $(1-4\sin^2\theta_W)$, to which the relevant (VEM-ANC) interference response function is proportional, makes experiments of this type extremely difficult.

In order to obtain more detailed information on the energy dependence of the $R_{\alpha\beta}(q,\omega)$ response, we employ the maximum-entropy method to invert $E_{\alpha\beta}(q,\tau)$. We describe the method here very briefly, several standard references are available [17,18] and a somewhat more expanded discussion of it is provided in Supplemental Material [2]. The numerical inversion of a Laplace transform $E_{\alpha\beta}(q,\tau)$ with its associated statistical errors is a notoriously ill-posed problem. The fact that we are interested in the (smooth) response around the quasielastic peak rather than isolated peaks makes it somewhat more practical. The maximum-entropy method is based on Bayesian statistical inference: the "most probable" response function is the one that maximizes the *posterior probability* $\Pr[R|\overline{E}\,]$, i.e., the conditional probability of R given $\overline{E}$. Bayes' theorem states that the posterior probability is proportional to the product $\Pr[\,\overline{E}|R\,]\times\Pr[R\,]$, where $\Pr[\,\overline{E}|R\,]$ is the *likelihood function* and $\Pr[R\,]$ is the *prior probability*. Arguments based on the central limit theorem show that the asymptotic limit of the likelihood function is given by $\Pr[\,\overline{E}|R\,]\propto\exp(-\chi^2/2)$ with χ^2 defined as follows. Let N_τ and N_ω be the numbers of grid points in the variables τ and ω, respectively. Then the Laplace transform in Eq. (2) reads [the q dependence and subscripts $\alpha\beta$ of $E_{\alpha\beta}(q,\tau)$ and $R_{\alpha\beta}(q,\tau)$ are suppressed for simplicity hereafter]

$$E_i=\sum_{j=1}^{N_\omega}K_{ij}\,R_j, \tag{4}$$

where $K_{ij}=\exp(-\tau_i\,\omega_j)$ and $R_j=\Delta\omega_j\,R(\omega_j)$, and the χ^2 follows from

$$\chi^2=\sum_{i,j=1}^{N_\tau}(\overline{E}_i-E_i)(C^{-1})_{ij}(\overline{E}_j-E_j), \tag{5}$$

where the E_i are obtained from Eq. (4), the $\overline{E}_i$ are the GFMC calculated values, and C is the covariance matrix. Therefore, maximizing the likelihood function reduces to finding a set of R_i values that minimizes the χ^2. The GFMC errors on $\overline{E}_i$ are strongly correlated in τ, as individual steps involve only small spatial distances and evolutions of the spin-isospin amplitudes. It is therefore of paramount importance to estimate the covariance matrix C.

Limiting ourselves only to the χ^2 minimization would implicitly be making the assumption that the prior probability is either unimportant or unknown. However, since the response function is positive definite and normalizable, it can be interpreted as yet another probability function. The *principle of maximum entropy* states that the values of a probability function are to be assigned by maximizing the entropy

$$S=\sum_{i=1}^{N_\omega}[R_i-M_i-R_i\ln(R_i/M_i)], \tag{6}$$

where $M_i=\Delta\omega_i\,M(\omega_i)$ and the positive definite function $M(\omega)$ is the *default model*. It is worthwhile mentioning that the above expression is applicable even when $R(\omega)$ and $M(\omega)$ have different normalizations. The entropy measures how much the response function differs from the model. It vanishes when $R(\omega)=M(\omega)$, and is negative when $R(\omega)\neq M(\omega)$. The maximum-entropy method adds to the simple χ^2 minimization the use of the prior information that the response function can be interpreted as a probability distribution function. We employ *historic maximum entropy* by minimizing $\alpha\,S-\chi^2/2$ with the parameter α adjusted to make the χ^2 equal to unity. While more refined methods relying on Bayesian statistical inference have been developed, we found historic maximum entropy to be simple to implement and adequate for our purposes.

As a first case we consider the electromagnetic response of ^{4}He. We generated a set of $N_E\simeq 2500$ GFMC estimates of the Euclidean response functions, obtained from independent imaginary-time propagations, on a grid of τ points uniformly distributed between 0 and 0.05 MeV^{-1} with $\Delta\tau=0.0005$ MeV^{-1}. The estimates were each started from statistically uncorrelated sets of 20 000 VMC configurations. Let $E_i^{(n)}=E^{(n)}(\tau_i)$ be the Euclidean response function corresponding to the nth GFMC propagation. The average Euclidean response function and covariance matrix elements are given by

$$\overline{E}_i=\frac{1}{N_E}\sum_{n=1}^{N_E}E_i^{(n)}, \tag{7}$$

$$C_{ij}=\frac{1}{N_E(N_E-1)}\sum_{n=1}^{N_E}\big[\overline{E}_i-E_i^{(n)}\big]\big[\overline{E}_j-E_j^{(n)}\big]. \tag{8}$$

In general, the covariance matrix is nondiagonal because of correlations between different τ_i, and the full expression for the χ^2 in Eq. (5) has been used (more details are given in the Supplemental Material [2]).

The ^{4}He longitudinal and transverse response functions (at $q=600$ MeV), obtained from inversion of $E_L(q,\tau)$ and $E_T(q,\tau)$, are shown in Fig. 3. The inversions are, to a

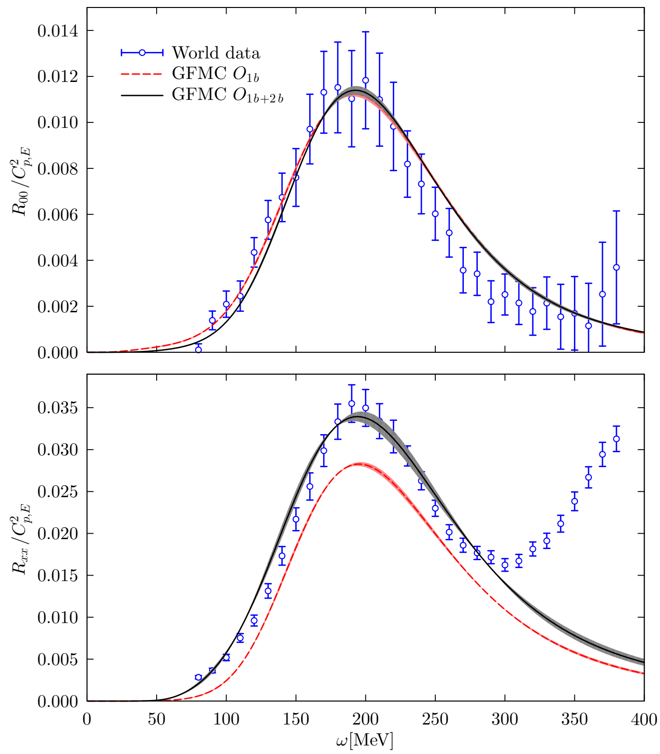

FIG. 3. (Color online) Electromagnetic longitudinal (top panel) and transverse (lower panel) response functions of ^{4}He at $q = 600$ MeV. Experimental data are from Ref. [11].

very large degree, insensitive to the choice of default model response [27]. Results obtained with one-body only (dashed line) and (one + two)-body (solid line) currents are compared with an analysis of the experimental world data [11] (empty circles). There is excellent agreement between the full theory and experiment. Two-body currents significantly enhance the transverse response function, not only in the dip region, but also in the quasielastic peak and threshold regions, providing the missing strength needed to reproduce the experimental results. An even larger enhancement in the transverse response occurs at $q = 300$ MeV [27], consistent with expectations from sum rule calculations [4].

Following Ref. [18], in order to study the sensitivity of the solution on the choice of the prior, we have used two noninformative default models: the flat model

$$M(\omega) = \alpha\, \theta(\omega_M - \omega), \tag{9}$$

where $\theta(\omega)$ is the step function and $\omega_M = 2$ GeV, and a simple Gaussian

$$M(\omega) = \alpha\, e^{-\omega^2/\sigma^2}. \tag{10}$$

In spite of the fact that the maximum-entropy algorithm turns out to be insensitive to the choice of the normalization constant, we have fixed α so that the the integral of the prior corresponds to the sum rule, the value of the Euclidean response function at $\tau = 0$. In the case of the Gaussian, the smallest possible σ compatible with $\chi^2 = 1$ is selected. The band in Fig. 3 provides an estimate of the dependence of the full results on the adopted default model. The model dependence is quite small.

With the exception of the leading relativistic corrections contained in the nuclear electroweak currents (see Ref. [1]), the present calculations are based on a nonrelativistic approach. Naive kinematical considerations would lead one to expect the quasielastic peak position in Fig. 3 to be at $q^2/(2\,m) + \Delta E \simeq 211$ MeV for $q = 600$ MeV—we take $\Delta E \simeq 20$ MeV to be the separation energy of ^{4}He into a $3+1$ cluster. The calculated response functions appear to peak at lower ω, in fact close to $\omega_{\rm qe} + \Delta E \simeq 195$ MeV. The width of the quasielastic peak is also seen to be correctly reproduced—the nonrelativistic Fermi gas fails to predict this quantity at momentum transfers $q \sim 600$ MeV as in Fig. 3. Thus, even at these relatively high momentum and energy transfers, the nonrelativistic dynamical framework adopted here may be more robust than comparisons between nonrelativistic and relativistic Fermi gas models would lead one to conclude [30].

A direct evaluation of the ^{12}C response functions via these same methods and with the same accuracy as the one of ^{4}He shown in Fig. 3, would require about 100 million core hours. We are examining improved methods including the use of correlated sampling that could improve the efficiency of this inversion. We are also exploring methods to extend these results to larger nuclei.

On the basis of the present ^{4}He and ^{12}C calculations, a consistent picture of the electroweak response of nuclei emerges, in which two-body terms in the nuclear electroweak current are seen to produce significant excess transverse strength from threshold to the dip region and beyond. Such a picture is at variance with the conventional one of inclusive quasielastic scattering, in which single-nucleon knockout is expected to be the dominant process in this regime.

We thank I. Sick for providing us with the data on the response functions of ^{4}He and ^{12}C. Useful discussions with O. Benhar, J. Gubernatis, and N. Rocco are also gratefully acknowledged. This research is supported by the US Department of Energy, Office of Science, Office of Nuclear Physics, under Contracts No. DE-AC02-06CH11357 (A.L. and S.C.P.), No. DE-AC02-05CH11231 (S.G. and J.C.), and No. DE-AC05-06OR23177 (R.S.), the NUCLEI SciDAC program, and by the LANL LDRD program. Under an award of computer time provided by the INCITE program, this research used resources of the Argonne Leadership Computing Facility at Argonne National Laboratory, which is supported by the Office of Science of the U.S. DOE under contract DE-AC02-06CH11357. We also used resources provided by Los Alamos Open Supercomputing and Argonne's LCRC, and by the National Energy Research Scientific Computing Center, which is supported by the Office of Science of the U.S. DOE under Contract No. DE-AC02-05CH11231.

[1] G. Shen, L. E. Marcucci, J. Carlson, S. Gandolfi, and R. Schiavilla, Phys. Rev. C **86**, 035503 (2012).

[2] See Supplemental Material at http://link.aps.org/supplemental/10.1103/PhysRevC.91.062501 for technical description of the

maximum entropy algorithm and for the explicit expressions for the electromagnetic and neutral-current transition operators used in our work.
[3] O. Benhar, Nucl. Phys. B, Proc. Suppl. **229-232**, 174 (2012).
[4] A. Lovato, S. Gandolfi, R. Butler, J. Carlson, E. Lusk, S. C. Pieper, and R. Schiavilla, Phys. Rev. Lett. **111**, 092501 (2013).
[5] A. Lovato, S. Gandolfi, J. Carlson, S. C. Pieper, and R. Schiavilla, Phys. Rev. Lett. **112**, 182502 (2014).
[6] O. Benhar, A. Lovato, and N. Rocco, arXiv:1312.1210.
[7] M. Martini, M. Ericson, G. Chanfray, and J. Marteau, Phys. Rev. C **80**, 065501 (2009).
[8] M. Martini, M. Ericson, G. Chanfray, and J. Marteau, Phys. Rev. C **81**, 045502 (2010).
[9] J. Nieves, I. R. Simo, and M. J. V. Vacas, Phys. Rev. C **83**, 045501 (2011).
[10] J. Amaro, M. Barbaro, J. Caballero, T. Donnelly, and C. Williamson, Phys. Lett. B **696**, 151 (2011).
[11] J. Carlson, J. Jourdan, R. Schiavilla, and I. Sick, Phys. Rev. C **65**, 024002 (2002).
[12] D. Gazit and N. Barnea, Phys. Rev. Lett. **98**, 192501 (2007).
[13] W. Leidemann and G. Orlandini, Prog. Part. Nucl. Phys. **68**, 158 (2013).
[14] S. Bacca, N. Barnea, W. Leidemann, and G. Orlandini, Phys. Rev. Lett. **102**, 162501 (2009).
[15] J. Carlson and R. Schiavilla, Phys. Rev. Lett. **68**, 3682 (1992).
[16] J. Carlson and R. Schiavilla, Phys. Rev. C **49**, R2880(R) (1994).
[17] R. Bryan, Eur. Biophys. J. **18**, 165 (1990).
[18] M. Jarrell and J. Gubernatis, Phys. Rep. **269**, 133 (1996).
[19] R. B. Wiringa, V. G. J. Stoks, and R. Schiavilla, Phys. Rev. C **51**, 38 (1995).
[20] S. C. Pieper, AIP Conf. Proc. **1011**, 143 (2008).
[21] J. Carlson and R. Schiavilla, Rev. Mod. Phys. **70**, 743 (1998).
[22] J. Carlson, S. Gandolfi, F. Pederiva, S. C. Pieper, R. Schiavilla, K. E. Schmidt, and R. B. Wiringa, arXiv:1412.3081.
[23] J. Carlson, Phys. Rev. C **36**, 2026 (1987).
[24] J. Jourdan, Nucl. Phys. A **603**, 117 (1996).
[25] E. Lusk, S. Pieper, and R. Butler, SciDAC Rev. **17**, 30 (2010), library available at http://www.cs.mtsu.edu/∼rbutler/adlb/.
[26] C. Adams, D. Adams, T. Akiri, T. Alion, K. Anderson, C. Andreopoulos, M. Andrews, I. Anghel, J. C. Costa dos Anjos *et al.* (LBNE Collaboration), arXiv:1307.7335.
[27] A. Lovato, S. Gandolfi, J. Carlson, S. C. Pieper, and R. Schiavilla (unpublished).
[28] R. Schiavilla and R. B. Wiringa, Phys. Rev. C **65**, 054302 (2002).
[29] L. E. Marcucci, M. Piarulli, M. Viviani, L. Girlanda, A. Kievsky, S. Rosati, and R. Schiavilla, Phys. Rev. C **83**, 014002 (2011).
[30] A. D. Pace, M. Nardi, W. Alberico, T. Donnelly, and A. Molinari, Nucl. Phys. A **726**, 303 (2003).